ISSN: 2249 –4820

Chemistry & Biology Interface, 2011, 1, 1, 135-160

Chemistry & Biology Interface

An official Journal of ISCB, Journal homepage; www.cbijournal.com

Research Article

Design and synthesis of new metal based potent chemotherapeutic agents derived from 3-acetoacetyl-7-methyl-pyrano-[4,3-b]-pyran-2,5-dione: DNA binding profile and *in vitro* cytotoxic activity against different human cancer cell lines

Farukh Arjmand[a]*, Mubashira Aziz[a]

[a]*Department of Chemistry, Aligarh Muslim University, Aligarh, 202002, Uttar Pradesh, India.*
Received 27 July 2011; Accepted 16 August 2011

Keywords: Macrocyclic complexes; DNA binding studies; pBR322 DNA; cleavage; cytotoxicity activity.

Abstract: New macrocyclic complexes of Co(II) (**1**), Cu(II) (**2**) and Zn(II) (**3**) derived from 3-acetoacetyl-7-methyl–pyrano-[4,3-b]-pyran-2,5-dione **(L)** were synthesized and characterized by elemental analysis and spectroscopic techniques. *In vitro* DNA binding studies of the ligand **L** and the complexes **1**-**3** were investigated by electronic absorption and emission titrations. The specific binding mode of **1**-**3** with 5'GMP was further validated by absorption and NMR spectroscopy. The complexes **1** and **2** also exhibited moderate cleavage activity against supercoiled plasmid pBR322 DNA. *In vitro* cytotoxicity results demonstrated that the highest growth inhibition was shown by **1**, while **3** displayed selectivity against Colo205 and MCF7 cancer cell lines. The ligand **L** and complex **2** were cytostatic as the cell viability remains constant.

1. Introduction

Design of metal-based cancer chemotherapeutic agents that target specific sequences of DNA could not only offer an optimal cure to this deadly disease but can be utilized by tuning/modulating the molecules by catering to the specific phenotype of cancer etiologies. This can be addressed by trapping the metal ion in a ligand framework, which has pharmacologically active, desired and well-tailored pharmacophore [1]. In this manner, a single chemical entity can be developed that is able to modulate multiple targets simultaneously, possibly delivering superior efficacy against complex diseases [2]. In the case of metal-containing combination agents, the pharmaceutically active ligand must either have an endogenous metal

* *Corresponding author: Tel.: +91 5712703893*
E-mail address: farukh_arjmand@yahoo.co.in

ISSN: 2249 –4820

Chemistry & Biology Interface, 2011, 1, 1, 135-160

binding function, or an appended ligating moiety to form the complex. Structure-activity relationship clearly demonstrate that substituting the organic functional groups or introduction of side chains/linkers can result in cell line specificity in addition to greater potency in terms of IC_{50} values [3-6]. For example, introduction of one or two flexible aminoalkyl substituents on the chromophore nucleus results in an improvement of the antiproliferative activity of pyranoderivatives–an important class of anticancer drugs for leukemia and human solid tumour HT-29 cell lines [7]. Coumarin derived analogues viz., butyrolactone and discodermolide are potent antiproliferative agents [8]. Coumarin, the basic molecule of the family of many derivatives, is the simplest naturally occurring phenolic substance possessing fused benzene and α-pyrone rings. The coumarins exist in a variety of forms, due to the various substitutions possible in their basic structure, which modulate their biological activity [9]. Coumarins are found in a number of natural products including the antibiotic novobicin, which inhibits DNA gyrase, and more recently have been shown to exhibit antitumour activity [10,11]. A series of natural and synthetic nitro and hydroxylated derivatives of coumarins have shown anti-proliferative activity by modulation of key biochemical pathways [12]. Complexes bearing coumarin functionality can be employed to design site-specific antitumour agents, which are selective for solid malignant cells with reduced toxicity [13,14]. To improve the pharmacological profile of the established antineoplastic agents, a number of platinum based coumarin complexes were synthesized and evaluated for their *in vitro* antiproliferative activity by Kokotos *et al* [15]. Additionally, the *in vitro* cytotoxicity of coumarin complexes of cerium, using Burkitt lymphoma (P3HR1) and leukemic (THP-1) cell lines were investigated by Manalov *et al* [16]. They found that complexation resulted in a 40% increase in cytotoxicity, compared to the metal-free ligand. To design a metal-based applicable anticancer drug, macrocyclic ligands hold promise as they are rigid enough to provide metal binding sites and orient functional groups stereoselectively, yet flexible enough to accommodate structural changes required for induced fit recognition of biological targets [17]. Enlightened by the aforementioned anticancer properties of metal-based derivatives of coumarins, we attempted to synthesize new potent antitumour coumarin based macrocyclic complexes of the biocompatible late 3d-transition metal ions viz; Co(II), Cu(II) and Zn(II). Being essential elements they may be less toxic than non-essential metal ions such as platinum. It has been well established that copper plays a crucial role in cell physiology as a catalytic cofactor in the redox chemistry of mitochondrial respiration, free radical scavenging and DNA synthesis [18]. Moreover, elevated levels of copper have been found in many types of human cancers and a specific amount of local copper appears to be required for angiogenesis to occur [19]. Therefore, a number of copper complexes have been screened for their anticancer activity and some of them were found to be active both *in vivo* and *in vitro* [18]. Cobalt is a bioessential element present in the active center of vitamin B12 which regulates the synthesis of DNA indirectly. Many biologically active cobalt complexes have been synthesized, showing antiproliferative, antimicrobial, antifungal and antiviral activity [20]. The ligand of our interest was 3-acetoacetyl-7-methyl-pyrano-[4,3-b]-pyran-2,5-dione which constitutes the lactone side chain and a 2,5-β-diketonate functional group. This ligand was combined to diaminocyclohexane to give Schiff base type macromolecule. In comparison to

ISSN: 2249 –4820
Chemistry & Biology Interface, 2011, 1, 1, 135-160

butyrolactone, the 7-hydroxyl group is eliminated which is not required for activity while diketo group facilitates macrocyclization and subsequent metal chelation. The *in vitro* binding studies of the coumarin ligand **L** and complexes **1-3** to the DNA−the primary pharmacological target of many anticancer drugs [21] have been performed by spectroscopic techniques. Furthermore, cytotoxicity activity of ligand and complexes were ascertained against a panel of human cancer cell lines.

2. Materials and methods

2.1. Chemistry

2.1.1. Materials

Reagent grade chemicals were used without further purification for all syntheses. $Co(ClO_4)_2.6H_2O$, $Ni(ClO_4)_2.6H_2O$, $Cu(ClO_4)_2.6H_2O$ and $Zn(ClO_4)_2.6H_2O$, *rac*-1,2- diaminocyclohexane, triethylorthoformate and dehydroacetic acid (Fluka) were used as received. Disodium salt of calf thymus DNA (highly polymerized stored at 4 °C), guanosine-5'-monophosphatedisodium salt (5'-GMP), tris(hydroxymethyl)aminomethane, agarose, ascorbic acid, sodium azide (NaN_3), DMSO, superoxide dismutase (SOD), H_2O_2, methyl green, DAPI (Sigma-Aldrich) and pBR322 supercoiled plasmid DNA (Genei, Bangalore) were used as received.

2.1.2. Physical measurements

Microanalysis (%CHN) was performed on a Perkin Elmer elemental analyzer model 2400. Molar conductances were measured at room temperature with a Eutech Instruments CON 510 digital conductometer. Infrared spectra were collected by using KBr pellets on a Perkin Elmer spectrum RX-1 FT-IR spectrometer. ^1H and ^{13}C spectra were recorded on a Bruker Avance-II spectrometer at 400 MHz and 100 MHz, respectively. Chemical shifts were reported on the δ scale in parts per million (ppm). The EPR spectrum of the copper complex was acquired on a Varian E 112 spectrometer using X-band frequency (9.1GHz) at liquid nitrogen temperature in solid state. The electrospray mass spectra were recorded on a Micromass Quattro II triple quadrupol mass spectrometer. Emission spectra were recorded with a Hitachi F-2500 fluorescence spectrophotometer. Cleavage experiments were performed with the help of Axygen electrophoresis supported by Genei power supply with a potential range of 50-500 Volts, visualized and photographed by Vilber-INFINITY gel documentation system.

2.2. DNA binding experiments

All the experiments involving the interaction of the complexes with CT DNA were conducted in aerated 5 mM Tris-HCl/50 mM NaCl buffer at pH 7.2. Solutions of calf thymus DNA in buffer gave a ratio of UV absorbance at 260 and 280 nm of ca. 1.9:1 indicating that DNA was free from protein [22]. DNA concentration per nucleotide was determined by the extinction coefficient 6600 $dm^3mol^{-1}cm^{-1}$ at 260 nm. Absorption spectral titration experiments were performed by maintaining a constant concentration of the ligand **L** and the complexes **1-3** and varying the nucleic acid concentration. This was achieved by diluting an appropriate amount of the ligand/complex solutions and DNA stock solutions while maintaining the total volume constant. This results in a series of solutions with varying concentrations of DNA but a constant concentration of the compound. The absorbance (A) was recorded after successive additions of CT DNA on

ISSN: 2249 –4820

Chemistry & Biology Interface, 2011, 1, 1, 135-160

Shimadzu UV-1700 pharmaspec UV/vis spectrophotometer using cuvettes of 1 cm path length. While measuring the absorption spectra an equal amount of DNA was added to both the compound solution and the reference solution to eliminate the absorbance of the DNA itself. The intrinsic binding constant K_b of the complex to CT DNA was determined from the eq (1) [23] through a plot of [DNA]/($\varepsilon_a - \varepsilon_f$) *vs*. [DNA]

$$[DNA]/(\varepsilon_a - \varepsilon_f) = [DNA]/(\varepsilon_b - \varepsilon_f) + 1/K_b(\varepsilon_b - \varepsilon_f) \quad (1)$$

Where [DNA] is the concentration of DNA in base pairs, ε_a, ε_f and ε_b are the apparent extinction coefficient (A_{obs}/[M]), the extinction coefficient of the free metal (M) complex and the extinction coefficient for the metal (M) complex in the fully bound form, respectively. In plots of [DNA]/(ε_a–ε_f) vs. [DNA], K_b is given by the ratio of the slope to the intercept. Fluorescence spectral measurements were carried out using Hitachi F-2500 spectrofluorometer. The Tris-buffer was used as a blank to make preliminary adjustments. The excitation wavelength was fixed and the emission range was adjusted before measurements. Fixed amount of ligand **L** and the complexes **1-3** were treated with increasing amount of CT DNA in 5 mM Tris-HCl/50 mM NaCl buffer. The concentration of the free metal complex was obtained from the equation;

$$C_f = C_t(F/F_0 - P)(1-P) \quad (2)$$

Where C_f is the free probe concentration, C_t is the total concentration of the probe added, F and F_0 are fluorescence intensities in presence and in the absence of CT DNA, respectively and P is the ratio of the observed fluorescence quantum yield of the bound probe to that of the free probe. The value of P was obtained from the intercept by extrapolating a plot of F/F_0 *vs.* 1/[DNA]. Binding data were plotted from the Scatchard equation of the form;

$$r/C_f = K(n-r) \quad (3)$$

r denotes ratio of C_b (=C_t-C_f) i.e., the bound probe concentration to the DNA concentration, K is the binding constant and n is the binding site number [24,25]. From the plot of r/C_f *vs.* r the binding constant K and binding site number n were obtained from the values of slope and intercept, respectively.

2.3. DNA cleavage

Cleavage experiments of supercoiled plasmid pBR322 DNA (300 ng) by complex **1** and **2** (10.0-70.0 μM) in 5mM Tris-HCl/50 mM NaCl, buffer at pH 7.2 were carried out and the reaction followed by agarose gel electrophoresis. The samples were incubated for 1h at 37 °C. A loading buffer containing 25% bromophenol blue, 0.25% xylene cyanol, 30% glycerol was added and electrophoresis was carried out at 50 V for 2h in Tris-HCl buffer using 1% agarose gel containing 1.0 μg/mL ethidium bromide. Reactions using pBR322 DNA in 5 mM Tris-HCl/50 mM NaCl buffer at pH 7.2 were treated with complex **1** and **2** (40.0 μM) and various radical inhibitors and/or activators such as ascorbic acid (Asc), DMSO, sodium azide (NaN_3), superoxide dismutase (SOD), H_2O_2; groove binders-methyl green and DAPI. The samples were incubated for 1h at 37 °C. The standard protocols were followed for these experiments [26,27].

2.4. In vitro anticancer assay

The cell lines used for *in vitro* antitumor screening activity were, MIAPaCa2, MCF7, ZR-75-1, SiHa, Colo205, HOP62, DWD, K562, DU145, A549, A498, T24, HCT15, HT 29, HeLa and PC3. These human

ISSN: 2249 –4820

Chemistry & Biology Interface, 2011, 1, 1, 135-160

malignant cell lines were procured and grown in RPMI-1640 medium supplemented with 10% fetal bovine serum (FBS) and antibiotics to study growth pattern of these cells. The proliferation of the cells upon treatment with the ligand **L** and the complexes **1-3** was determined using the sulphorhodamine-B (SRB) semi automated assay [28]. Cells were seeded in 96 well plates at an appropriate cell density to give optical density in the linear range (from 0.5 to 1.8) and were incubated at 37 °C in CO_2 incubator for 24 h. Stock solution of the compounds was prepared as 100 mg/mL in DMSO and four dilutions i.e. 10 µL, 20 µL, 40 µL, 80 µL, in triplicates were tested, each well receiving 90 µL of cell suspension and 10 µL of the drug solution. Appropriate positive control (adriamycin) and vehicle controls were also run. The plates with cells were incubated in CO_2 incubator with 5% CO_2 for 24 hours followed by drug addition. The plates were incubated further for 48 h. Termination of experiment was done by gently layering the cells with 50 µL of chilled 30% TCA (in case of adherent cells) and 50% TCA (in case of suspension cultures) for cell fixation and kept at 4 °C for 1h. Plates were washed, air-dried and stained with 50 µL of 0.4% SRB in 1% acetic acid for 20 min. The bound SRB was eluted by adding 100 µL 10 mM Tris (pH 10.5) to each of the wells. The absorbance was read at 540 nm with 690 nm as reference wavelength. All experiments were repeated 3 times.

3. Synthesis

3.1. Synthesis of 3-acetoacetyl-7-methyl – pyrano-[4,3-b]- pyran-2,5- dione, ***L***

The ligand **L** was synthesized by a procedure as reported elsewhere [29].

3. 2. General procedure for the synthesis of macrocyclic complexes, ***1-3****.*

To a solution of an appropriate metal perchlorate (5.00 mmol) in 20 mL of methanol, 1.22 mL (10.00 mmol) of *rac*-1,2-diaminocyclohexane was added dropwise. The reaction mixture was stirred at 35 °C for 30 minutes and then 2.62 g (10.00 mmol) of ligand **L** dissolved in 30 mL of methanol was added, stirred for additional 1 h and heated under reflux for 6 h until peculiar color changes were observed. The reaction mixture was filtered and the filtrate was reduced under vacuum to remove the excess solvent. The product obtained was purified by repeated recrystallization from MeOH/$CHCl_3$ and air dried.

3.2.1. Analytical data for complex $C_{38}H_{44}N_4O_{18}Cl_2Co$, (***1***)

Yield: 42.2%, Colour: reddish brown; M.Pt. 280 °C; Anal. calc. for $C_{38}H_{44}N_4O_{18}Cl_2Co$; C 46.83, H 4.55, N 5.75; found C 46.77, H 4.67, N 5.64; IR (KBr, cm^{-1}) 1685 $\nu(C=O)_{lactonic}$; 1649 $\nu(C=N)$; 1619 $\nu(C=O)$; 1474 $\delta(CH_2)_{dach}$; 2934, 2861 $\nu(CH_2)_{dach}$; 3431 $\nu(NH+OH)$; 3085 $\nu(=CH)_{vinyl}$; 589 $\nu(Co-N)$; 550 $\nu(Co-O)$: UV/vis (DMF, 10^{-3}, 25 °C, nm) 255, 340, 520. ESI MS, m/z 973.7 $[M]^+$, 959.0 $[M-H_2O]$, 937.8 $[M-2H_2O]$. Molar conductance (λ_M, Scm^2mol^{-1}, 10^{-3}, 25 °C, MeOH) 192.1 (1:2 electrolyte).

3.2.2. Analytical data for complex $C_{38}H_{44}N_4O_{18}Cl_2Cu$, ***(2)***

Yield: 39.0%, Colour: purple; M.Pt. 240 °C; Anal. calc. for $C_{38}H_{44}N_4O_{18}Cl_2Cu$; C 46.61, H 4.53, N 5.72; found C 46.59, H 4.50, N 5.68; IR (KBr, cm^{-1}) 1715, 1610 $\nu(C=O)_{lactonic}$; 1645 $\nu(C=N)$;1619 $\nu(C=O)$; 1467 $\delta(CH_2)_{dach}$; 2920, 2858 $\nu(CH_2)_{dach}$; 3487 $\nu(NH+OH)_{H2O}$; 3070 $\nu(=CH)_{vinyl}$; 567 $\nu(Cu-N)$; 539 $\nu(Cu-O)$.UV/vis ($CHCl_3$, 10^{-3}, 25 °C, nm) 252, 320, 588. ESI-MS, m/z 979.0 $[M]^+$, 961.2 $[M-H_2O]$, 942.7 [M-

ISSN: 2249 –4820

Chemistry & Biology Interface, 2011, 1, 1, 135-160

$2H_2O$]. Molar conductance (λ_M, Scm^2mol^{-1}, 10^{-3}, 25 °C, DMF) 142.5 (1: 2 electrolyte).

3.2.3. Analytical data for complex $C_{38}H_{44}N_4O_{18}Cl_2Zn$, (3)

Yield: 47.0%, Colour: Brown; M.Pt. 202 °C; Anal. calc. for $C_{38}H_{44}N_4O_{18}Cl_2Zn$; C 46.52, H 4.52, N 5.71; found C 46.56, H 4.47, N 5.85; IR (KBr, cm^{-1}) 1653 $\nu(C=O)_{lactonic}$; 1653 $\nu(C=N)$; 1612 $\nu(C=O)$; 1464 $\delta(CH_2)_{dach}$; 2935, 2861 $\nu(CH_2)_{dach}$; 3329 ν (NH+OH); 3120 $\nu(=CH)_{vinyl}$; 566 ν(Zn-N); 527 ν(Zn-O): UV/vis ($CHCl_3$, 10^{-3}, 25 °C, nm) 242, 320. Molar conductance (λ_M, Scm^2mol^{-1}, 10^{-3}, 25 °C, MeOH) 205.3 (1:2 electrolyte). ^1H NMR (δ $CDCl_3$, 400 MHz, 25 °C, ppm) 1.88-1.92, 1.96-2.18 $(CH_2)_{dach}$; 2.11-2.35 $(CH_3)_{acetyl}$; 2.44-2.54 $(CH_3)_{exo}$; 4.83-4.85 $(=CH)_{vinyl}$; 7.16, 8.14 $(CH)_{ring}$; 5.61-5.70 (-NH). ^{13}C NMR (δ $CDCl_3$, 100 MHz, 25 °C, ppm) 175.33 (C=N); 28.94, 24.38 (CH_3); 20.09 $(CH_2)_{dach}$; 162.64 $(C=O)_{ring}$. ESI-MS, m/z 981.2 $[M]^+$, 964.1 $[M-H_2O]$, 946.3 $[M-2H_2O]$.

4. Results and discussion

4.1. Chemistry

The macrocyclic Co(II) (**1**), Cu(II) (**2**) and Zn(II) (**3**) complexes were prepared *in situ* by refluxing a methanolic solution of metal perchlorates, diaminocyclohexane and the coumarin ligand 3-acetoacetyl-7-methyl–pyrano-[4,3-b]-pyran-2,5-dione (**L**) in a 1:2:2 molar ratio, respectively (Scheme 1. Synthesis of macrocyclic complexes). The synthesis of the ligand **L** has been reported elsewhere [29]. The complexes **1-3** were recrystallized from chloroform/methanol mixture and pure complexes were obtained by separating the compound by preparatory TLC ($CHCl_3/CH_3OH$, 95:5). The yield of the complexes was < 50%. The complexes are air stable and insoluble in water, sparingly soluble in MeOH, $CHCl_3$, readily soluble in DMSO and DMF. The repeated attempts to grow single crystals of X-ray quality failed. However, the formation of complexes was ascertained by elemental analysis, which serves as a basis for the determination of their empirical formulae, confirmed by IR spectroscopy, ^1H, ^{13}C NMR spectroscopy and mass spectral data. All these spectroscopic data support the presented formulae and the proposed structure of the complexes.

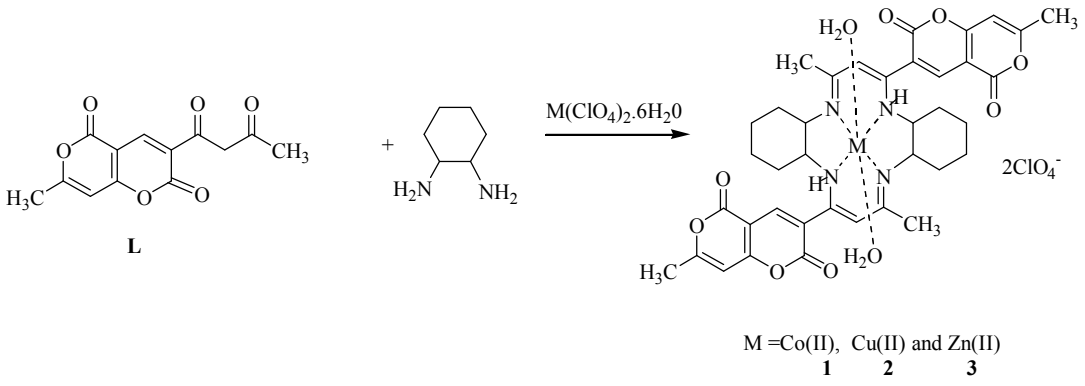

L

ISSN: 2249 –4820

Chemistry & Biology Interface, 2011, 1, 1, 135-160

4.2. Characterization

4.2.1. IR spectroscopy

IR spectra of the ligand **L** and the complexes **1-3** were recorded in solid state as KBr discs in the range 500-3800 cm^{-1}. The ligand **L** exhibits the characteristic stretching vibrations of the carbonyl groups of lactone rings at 1760 cm^{-1} and 1724 cm^{-1} and low frequency sharp band observed at 1626 cm^{-1} was assigned to stretching vibration of the –C=O of the β-diketonate residue which was in resonance with the lactone ring [30-32]. A broad band at 3431 cm^{-1} characteristic of ν(OH) vibration was attributed to the enolic OH vibrations implying that the ligand exhibits keto-enol tautomerisation [33,34]. This was confirmed by the presence of a vinylic ν(=CH) stretch at 3073 cm^{-1}. Other medium intensity bands in the range 1300-1400 cm^{-1} due to the in plane bending modes of ν(CH_3) and ν(=CH) groups were also observed. Absorption maxima found at 1554 cm^{-1} and 1197 cm^{-1} were attributed to the ν(C=C) and ν(C–O) stretching modes of the pyran rings, respectively. The IR spectra of the macrocyclic complexes **1-3** revealed some notable features. Disappearance of ν(C=O) at 1724 cm^{-1} and 1626 cm^{-1} and the appearance of a strong band in the range 1641-1653 cm^{-1} assigned to ν(C=N) provided strong evidence for the conversion of ketonic groups into the azomethine groups of the Schiff base residues [35]. The macrocyclic formation through Schiff base condensation was supported by the appearance of new bands in the range 2920-2935 cm^{-1} and 2857-2861 cm^{-1} due to symmetric and asymmetric ν(CH_2) vibrations of the dach moieties.

Additionally, the IR spectra of the complexes also display a wide band at 3329-3487 cm^{-1} associated with the stretching vibrations of the water molecules and the coordinated ν(NH) groups. This substantiates the fact that both the ligand and the metal complexes show tautomerism. However, bands belonging to –OH bending vibrations could not be assigned, owing to the overlay with very intense ν(C=N). The conclusive evidence for the coordination mode of metal complexes was deduced by the observation of new ν(M-N) bands around 513-527 cm^{-1} in the far IR region [36,37]. Similarly, the presence of uncoordinated perchlorate anions was depicted by the lack of splitting of ν(Cl-O) bands observed in the range 1055-1114 cm^{-1} and 624-649 cm^{-1} [38].

4.2.2. NMR Spectroscopy

The identification of ligand **L** and the metal complexes was further obtained from NMR spectroscopy. The ^{1}H NMR spectrum of the ligand **L** displayed a broad signal at 15.75 ppm, characteristic of enolic proton [39]. Peaks with chemical shifts near 6.25-8.76 ppm were ascribed to –C=CH and –CH=C-C ring protons. The signals for the alkyl –CH_3 protons and the vinylic =CH protons were detected at 2.09-2.31 ppm, 2.41-2.45 ppm and 4.09-4.12 ppm. Similar chemical shifts were observed for the corresponding protons in ^{1}H NMR spectra of the diamagnetic complex **3**. The –OH resonance disappears while a new peak at 5.61-5.70 ppm emerges due to the coordinated –NH proton. Additional peaks in the range 1.88-1.92 and 1.96-2.18 ppm absent in the spectrum of the ligand **L** was attributed to different cyclohexyl ring protons.

The ^{13}C NMR spectra of the ligand **L** and the complex **3** corroborated well with the proposed structures. In the spectrum of **L**, the ^{13}C NMR signals for the two lactonic carbonyl carbons appear at 156.13 and 159.31 ppm [40]. Resonance due to –C=O

ISSN: 2249 –4820

Chemistry & Biology Interface, 2011, 1, 1, 135-160

and =CH-OH of the diketone residue appear at 199 ppm and 168 ppm, respectively [41]. However, significant changes were observed in the spectrum of complex **3**. A new signal appeared at 175.33 ppm due to C=N, confirming the cyclization of the ligand with the dach moieties. Resonances at 20.09 and 24.38-28.94 were ascribed to the cyclohexyl ring carbons and the CH_3 groups, respectively. Other peaks remained almost undisturbed in the spectrum of complex **3**.

4.2.3. Electronic spectra

The electronic spectrum of the ligand **L** in DMF shows intense absorption bands at 279 nm and 385 nm. The strong bands appearing at the low energy side were assigned to n→ π* associated with the C=O group. The bands at the higher energy arise from π→ π* transitions within the lactonic rings or exocyclic carbonyl groups [42]. These absorption bands in complexes **1-3** were shifted to longer wave numbers. A prominent band at 320-341 nm was ascribed to n→ π* transition of the azomethine chromophore [43]. In the visible region, complexes **1** and **2** revealed bands at 520 nm and 588 nm ascribed to d-d transitions of the Co(II) and Cu(II) ions, respectively in an octahedral coordination geometry [44,45].

4.2.4. Mass spectroscopy

Electrospray ionization mass spectra of the ligand **L** and the metal complexes **1-3** were obtained to confirm their proposed molecular formulae. The ligand **L** displayed the molecular ion peak at m/z 262.3. The mass spectra of complexes **1-3** recorded molecular ion peaks at m/z 973.7, 979.0 and 981.2, respectively. Fragments obtained by the successive expulsion of the coordinated water molecules were also depicted in the mass spectra of the complexes **1-3**, supporting the proposed molecular formulae.

4.2.5. EPR spectrum

Solid state X-band EPR spectrum of the paramagnetic Cu(II) complex **2** obtained at LNT at 9.1 GHz, recorded an isotropic signal at 2.04 with the unpaired electron located in dz^2 orbital having an octahedral geometry [46].

5. In vitro DNA binding studies

DNA is generally regarded as the primary pharmacological target of many anticancer drugs, [47] which can bind with the DNA duplex mainly through covalent, non-covalent and electrostatic interactions. Among the non-covalent binding modes intercalation is an important binding mode as many naturally derived compounds are known to exhibit their anti-proliferative activity and apoptosis effect on tumor cells involving intercalation [48]. The DNA intercalators are required to possess an approximately planar structure, with a medium-sized planar area and some hydrophobic character. So, in order to evaluate the DNA binding propensity of the ligand and its metal complexes, we carried out various biophysical studies as described below.

5.1. Absorption titration with CT DNA

Electronic absorption spectroscopy is one of the most useful techniques for DNA binding studies of metal complexes. The absorption spectra of the ligand **L** and complexes **1-3** in the absence and presence of CT DNA are presented in Fig. 1-4. The ligand exhibits the absorption maxima at 279 nm and 385 nm attributed to π→π* and n→π* transitions, respectively. In presence of CT DNA, both the absorption bands exhibited

ISSN: 2249 –4820

Chemistry & Biology Interface, 2011, 1, 1, 135-160

hyperchromism and the band at 279 nm also undergoes a red shift (bathochromic shift) of 5 nm (Fig. 1). The hyperchromicity implies that some interaction other than intercalation has occurred between ligand and DNA, because intercalation would lead to hypochromism and bathochromic shift in UV absorption spectra [49]. It appears that the hyperchromism occurs due to the aggregation of the planar ligand molecules on the DNA surface and/or intimate surface binding of the lactone rings along the DNA backbone, resulting in the breakage of the secondary structure of DNA [50,51]. The intrinsic binding constant K_b for ligand to CT DNA was calculated to be 1.47 $\bullet 10^4$ M^{-1}, a value lower than that obtained for typical intercalator (EB-DNA $\approx 10^7$). The complex **2** exhibits intraligand transitions at 279 nm and 320 nm attributed to $\pi \rightarrow \pi^*$ and $n \rightarrow \pi^*$ transitions, respectively and a d-d transition maximum at 588 nm. In presence of CT DNA, there are interesting changes in absorption spectra. Unlike the ligand **L**, the complex exhibits hypochromism at 320 nm absorption band attributed to $n \rightarrow \pi^*$, while as the d-d transition at 588 nm undergoes hyperchromism with no red shift (Fig. 2). This pattern reveals that while the UV absorption band undergoes hypochromism suggesting that the complex has intimate association with CT-DNA and binds to the helix via the intercalative mode, [52,53] at the same time electrostatic interaction due to the presence of strong Lewis acid copper centre of the complex with the negatively charged phosphate backbone of the DNA helix cannot be ruled out which is evidenced by 'hyperchromism' of d-d absorption maxima [54-56].

Complexes **1** and **3** in a similar fashion to complex **2** recorded an initial hypochromism and then hyperchromism at the intraligand absorption bands (Fig. 3 & 4). The observed 'hypo' and 'hyperchromic' effects reveal that the complexes **1-3** possess more than one DNA binding mode. Also, the hypochromicity observed in our complexes is much weaker than reported in the literature [57]. The hypochromicity is mainly decided by the interaction between the electronic states of the planar chromophore and nucleobases which can stabilize the DNA duplex; stronger hypochromicity always indicates a larger binding strength towards DNA. We therefore, used the hypochromicity to calculate the quantitative binding affinity of the complexes **1-3** with DNA. The K_b values were found to be 3.63 $\bullet 10^4$ M^{-1}, 2.18 $\bullet 10^5$ M^{-1} and 2.72 $\bullet 10^4$ M^{-1} for **1**, **2** and **3,** respectively. The much larger K_b value of **2** in comparison to **1** and **3** suggested a stronger and multiple binding interactions between **2** and DNA double helix.

ISSN: 2249 –4820

Chemistry & Biology Interface, 2011, 1, 1, 135-160

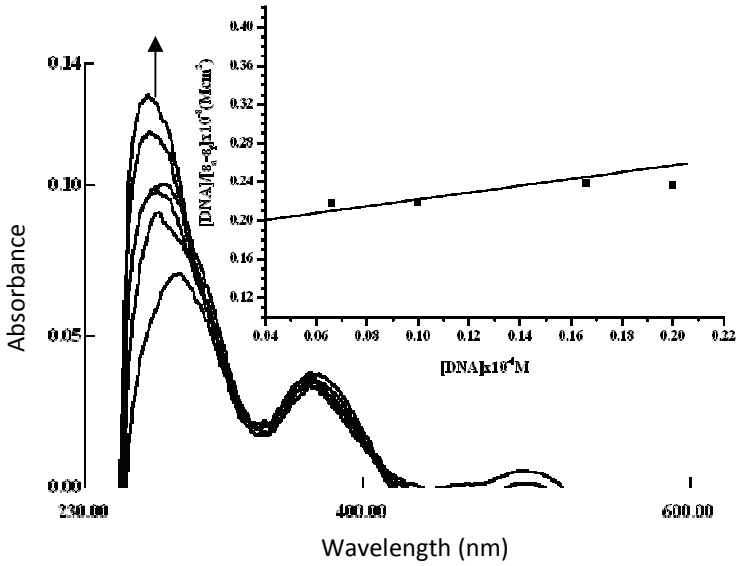

Figure 1

Absorption spectral traces of ligand **L** in 5 mM Tris-HCl/50 mM NaCl buffer upon addition of CT DNA. Arrow shows the absorbance change upon increasing concentration of the CT DNA. Inset: Plot of [DNA]/ ε_a-ε_f *vs* [DNA] for the titration of CT DNA with ligand **L**; [**L**] = 6.60 μM, [DNA] = 6.60-20.00 μM; (■) experimental data points; full lines, linear fitting of the data

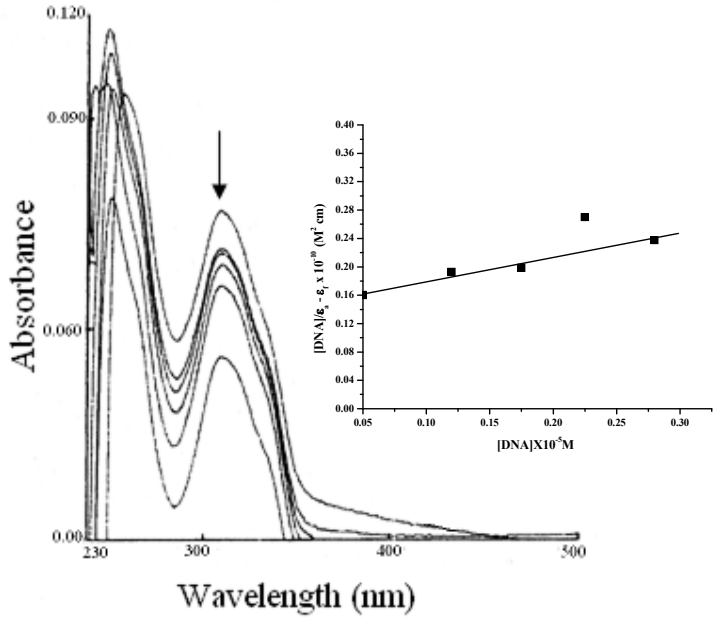

Figure 2

Absorption spectral traces of complex **2** in 5 mM Tris-HCl/50 mM NaCl buffer upon addition of CT DNA. Arrow shows the absorbance change upon increasing concentration of the CT DNA. Inset: Plots of [DNA]/ ε_a-ε_f *vs* [DNA] for the titration of CT DNA with complex; [Complex **2**] =

ISSN: 2249 –4820

Chemistry & Biology Interface, 2011, 1, 1, 135-160

1.60 μM, [DNA] = 0.55-2.77 μM; (■) experimental data points; full lines, linear fitting of the data

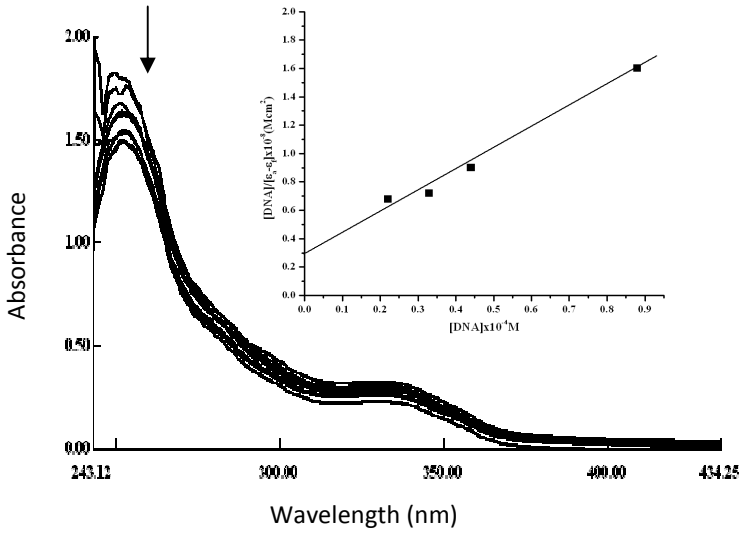

Figure 3

Fig. 3. Absorption spectral traces of complex **1** in 5 mM Tris-HCl/50 mM NaCl buffer upon addition of CT DNA. Arrow shows the absorbance change upon increasing concentration of the CT DNA. Inset: Plots of [DNA]/ ε_a-ε_f *vs* [DNA] for the titration of CT DNA with complex **1**; [Complex **1**] = 33.30 μM, [DNA] = 11.0-88.0 μM; (■) experimental data points; full lines, linear fitting of the data.

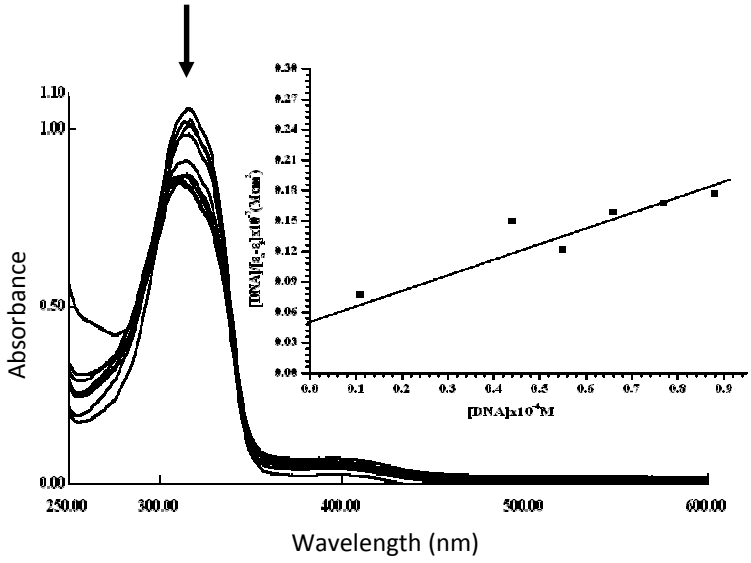

Figure 4

Fig. 4. Absorption spectral traces of complex **3** in 5 mM Tris-HCl/50 mM NaCl buffer upon addition of CT DNA. Arrow shows the absorbance change upon increasing concentration of the CT DNA. Inset: Plots of [DNA]/ ε_a-ε_f *vs* [DNA] for the titration of CT DNA with complex **3**;

ISSN: 2249 –4820

Chemistry & Biology Interface, 2011, 1, 1, 135-160

[Complex **3**] = 33.30 μM, [DNA] = 11.0-88.0 μM; (■) experimental data points; full lines, linear fitting of the data

5.2. Absorption titration with 5'GMP

To identify the specific DNA binding site/mode of the metal complexes **1**-**3**, interaction studies with the nucleotide 5′GMP were examined by absorption titration. The recognition of 5′GMP is crucial because it acts as an intermediate in the synthesis of nucleic acids and plays important roles in several metabolic pathways [58]. Late transition metal ions (borderline Lewis acids) are known to bind with the phosphate groups as well with the nitrogenous DNA bases [59]. The N7 of the guanine is considered as the dominant binding site [60,61]. On increasing the concentration of the nucleotide there was a sharp increase in intensity of the UV absorption bands of complexes **1** and **2**, while hypochromism was observed for complex **3** as shown in **Fig. 5**. 'Hyper' and 'hypochromism' at the UV absorption bands is thus, consistent with the DNA binding of the complexes involving hydrophobic interactions between the ligand and the DNA via partial intercalation and the electrostatic binding of the metal ions towards the sugar phosphate backbone [62]. No significant changes were observed at the d-d absorption maxima. Therefore, coordination of the central metal ions towards the N7 atom of guanine was precluded.

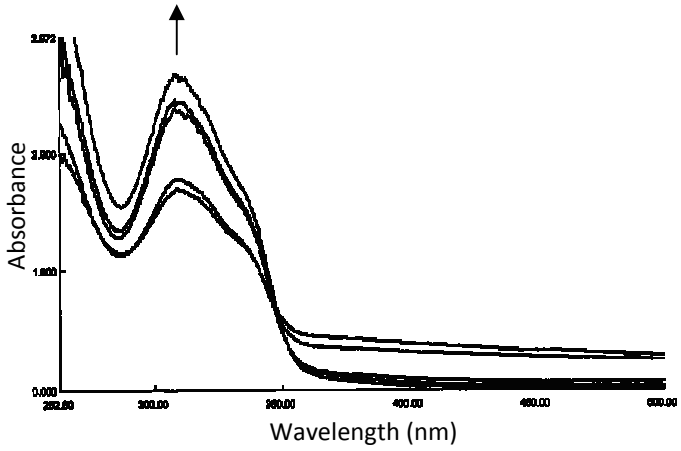

Figure 5a

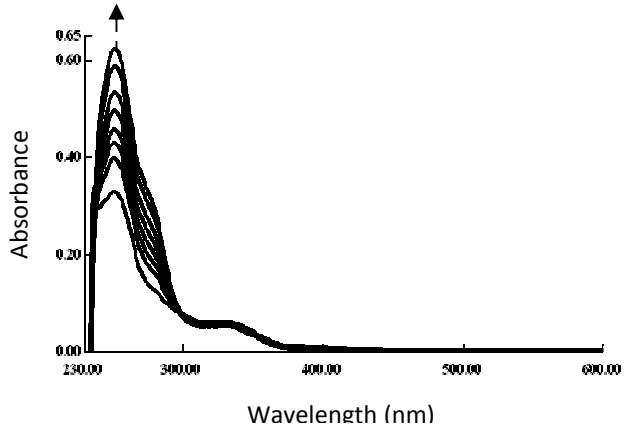

ISSN: 2249 –4820

Chemistry & Biology Interface, 2011, 1, 1, 135-160

Figure 5b

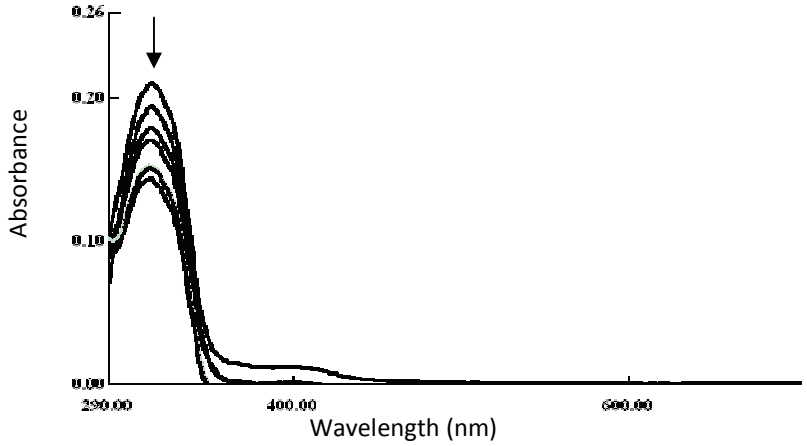

Figure 5c

Absorption spectral traces of a) complex **1** b) complex **2** c) complex **3** in 5 mM Tris-HCl/50 mM NaCl buffer upon addition of 5′GMP Arrows show the absorbance changes upon increasing concentration of the 5′GMP

5.3. ^{1}H and ^{31}P NMR studies with 5′GMP

The interaction of complexes **1-3** with guanosine-5′-monophosphate was evaluated by using ^{1}H and ^{31}P NMR technique. The ^{1}H NMR spectrum of 5′GMP in D_2O solvent recorded the proton resonance of guanine H8 at 8.10 ppm and ribose H1′-H5′ at 3.8-5.8 ppm, respectively. For paramagnetic complexes, the chemical shift of proton adjacent to the metal center will be perturbed resulting in line broadening. On interaction of complexes **1-3** with 5′GMP the H8 signal of guanine does not alter significantly (8.12 ppm) (**Fig. 6**). At different time intervals the spectra remained unaltered, revealing the non-participation of N7 of guanine in covalent binding with the metal ion [63].

Furthermore, there is line broadening of H8 and H1′-H5′ signals of ribose sugar which indicate the presence of paramagnetic Cu(II)/Co(II) center in the proximity of these protons. The ^{31}P NMR spectrum of 5′GMP reveals a signal at 3.67 ppm. Upon interaction of complexes **1-3** with 5′GMP, the resonance shifts upfield to 3.60 ppm indicative of electrostatic binding mode of the complexes to the phosphate group of 5′GMP. Since there is no large upfield shift, it implies that the complex involves other non-covalent DNA binding modes in addition to electrostatic binding. These observations are in corroboration with UV-vis and fluorescence spectral data.

ISSN: 2249 –4820

Chemistry & Biology Interface, 2011, 1, 1, 135-160

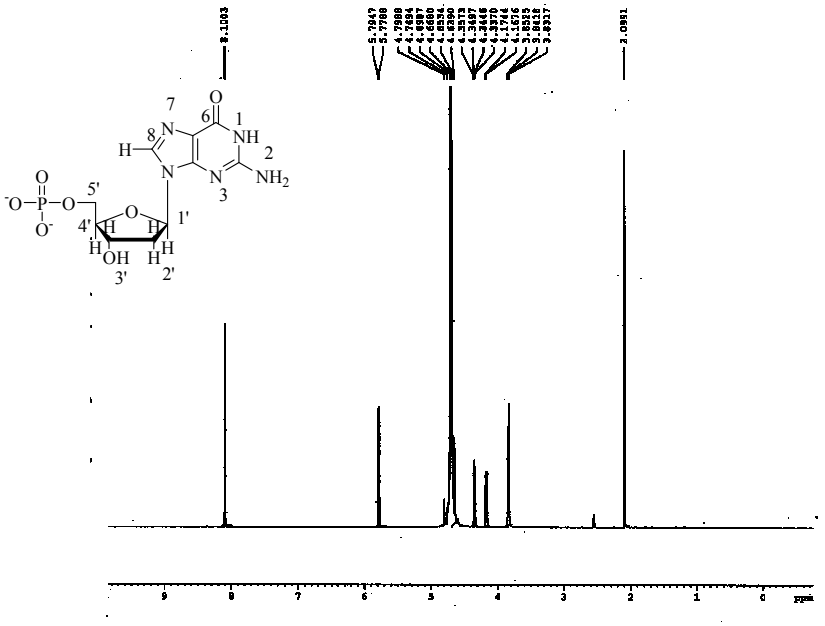

Figure 6a

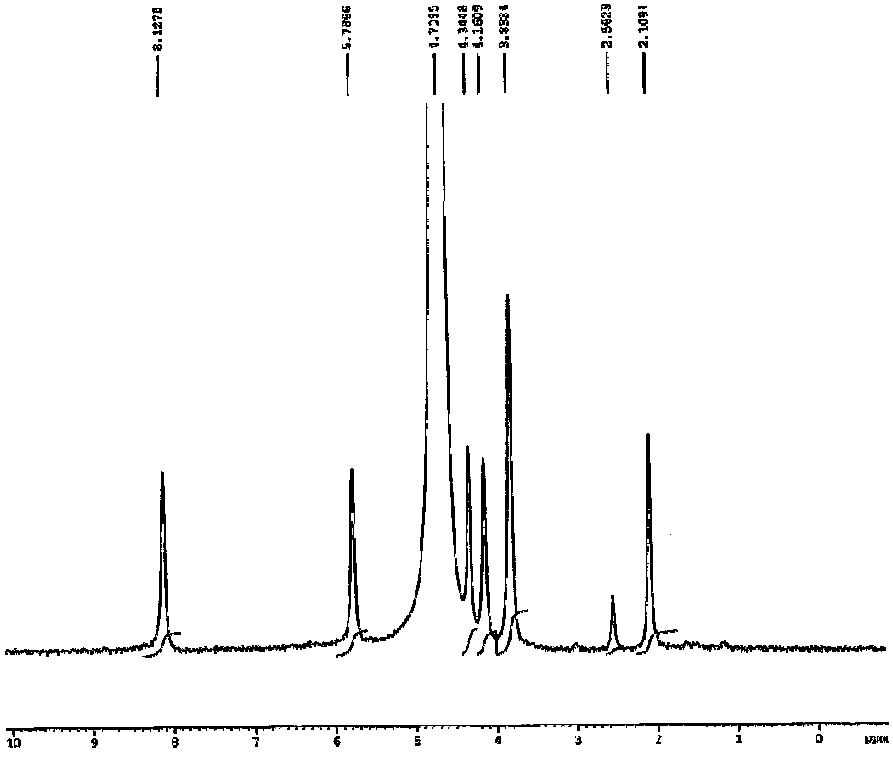

Figure 6b

^{1}H NMR spectra of a) 5′GMP and b) the reaction of complex **2** (2.5 mM) with 5′GMP (5 mM) in D_2O at 25 °C

ISSN: 2249 –4820

Chemistry & Biology Interface, 2011, 1, 1, 135-160

5.4. Emission titration

The ligand **L** and the complex **2** emit luminescence in Tris-buffer with a maximum appearing at 567 nm and 525 nm, respectively. Upon the addition of increasing concentrations of DNA, the emission intensity of both the ligand **L** and the complex **2** enhances gradually (**Fig. 7**). The emission enhancement is usually correlated with the extent to which the compounds penetrate into the hydrophobic pockets of DNA, thereby avoiding the quenching effects of solvent water molecules [64]. Due to the reduced solvent mobility at the binding site by the hydrophobic DNA macromolecule, a decrease in vibrational modes of relaxation results and hence quenching efficiency, especially in case of intercalation [65,66]. Our emission titration results, thus, support the idea that both the ligand as well as the complex are protected from the solvent water molecules and can insert deeply into the DNA helix [67]. However, complexes **1** and **3** can emit luminescence in Tris-HCl buffer around 450 nm at room temperature, when excited at 378 nm. The result of the emission titration for the complexes **1** and **3** upon addition of DNA is displayed in **Fig. 8.** The emission intensity decreases due to the collisional quenching mode of the complexes to CT DNA by the partial release of the coordinated H_2O molecules and deprotection by the whole complex [68]. To compare the binding affinity of the ligand and the complexes **1-3** the binding data obtained from the emission spectra were fitted in the Scatchard equation to acquire the binding parameters. A plot of r/C_f *vs.* r gave the binding constants as $3.00 \bullet 10^4$ M^{-1}, $1.51 \bullet 10^5$ M^{-1}, $6.50 \bullet 10^5$ M^{-1} and $6.0 \bullet 10^4$ M^{-1} for the ligand **L** and the complexes **1-3,** respectively.

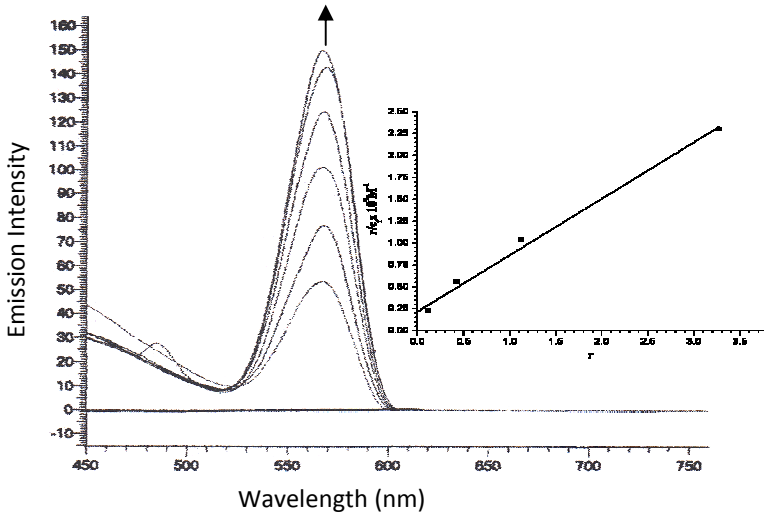

Figure 7a

ISSN: 2249 –4820

Chemistry & Biology Interface, 2011, 1, 1, 135-160

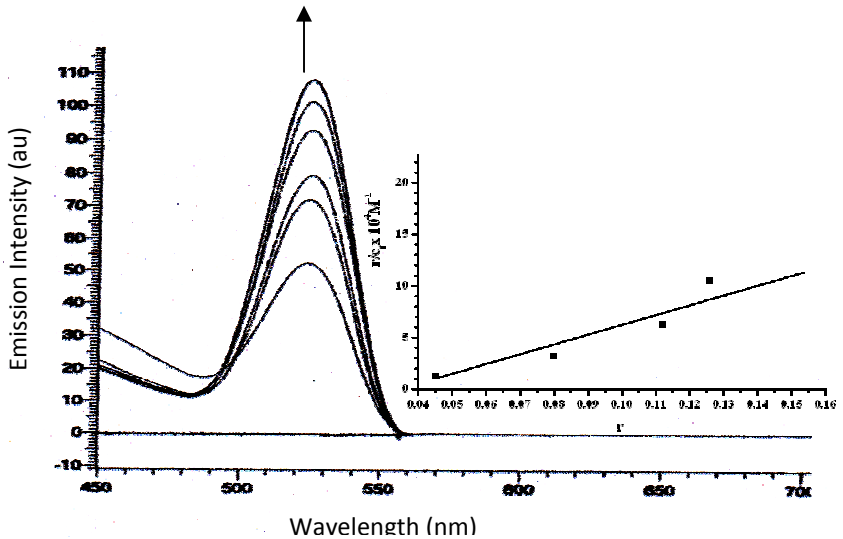

Figure 7b

Emission spectra of **a**) ligand **L** b) complex **2** in absence and presence of DNA in 5 mM Tris-HCl/50 mM NaCl buffer. Arrows show the intensity changes upon increasing concentration of the DNA. Inset: Plot of r/C_f *vs* r; [**L**/Complex **2**] = 3.30 μM, [DNA] = 3.30-16.60 μM; (■) experimental data points; full lines, linear fitting of the data

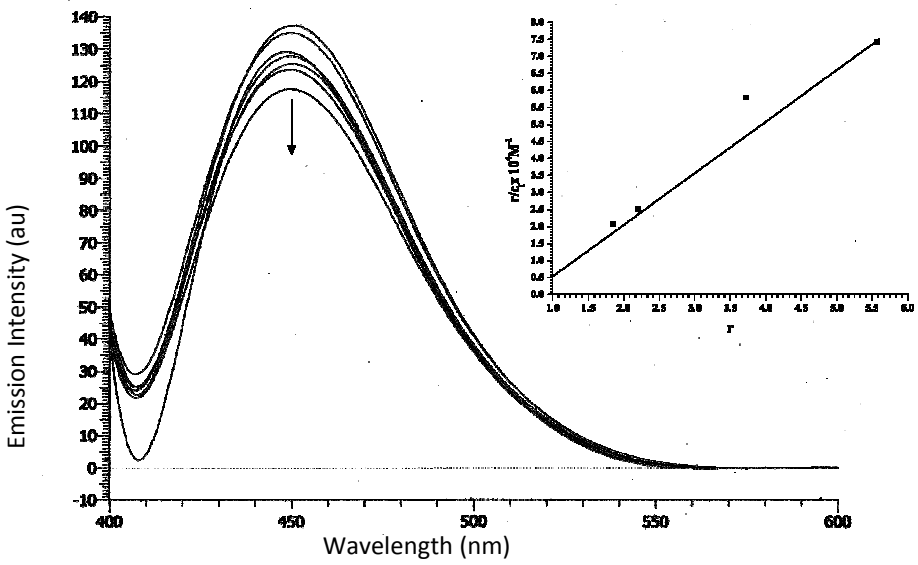

Figure 8a

ISSN: 2249 –4820

Chemistry & Biology Interface, 2011, 1, 1, 135-160

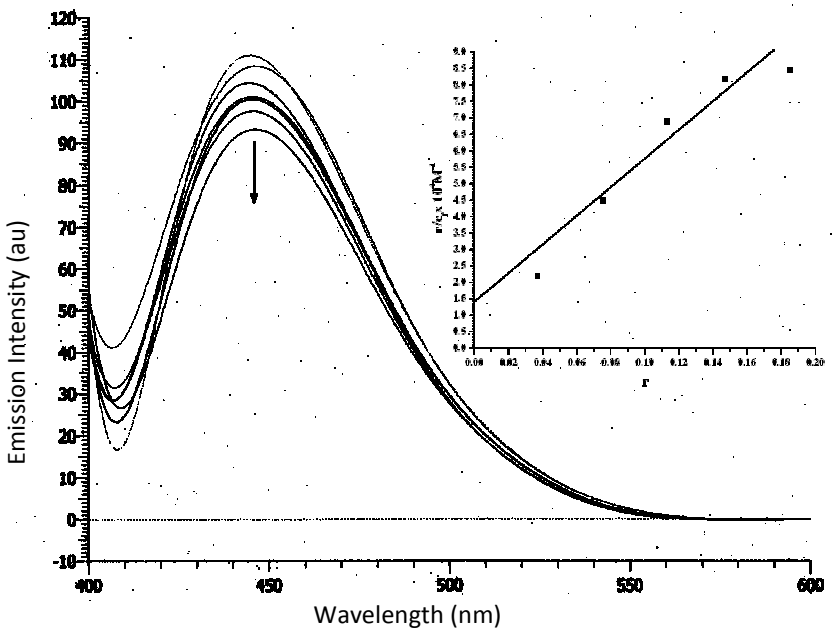

Figure 8b

Emission spectra of a) complex **1** b) complex **3** in absence and presence of DNA in 5 mM Tris-HCl/50 mM NaCl buffer. Arrows show the intensity changes upon increasing concentration of the DNA. Inset: Plot of r/C_f *vs* r; [Complex **1**/**3**] = 66.00 μM, [DNA] = 11.70-40.97 μM; (■) experimental data points; full lines, linear fitting of the data.

5.5. Competitive binding experiment

To have a better understanding of the binding mode of the ligand **L** and the complexes **1-3** with DNA a competitive binding experiment was carried out using EB as a probe. EB shows weak luminescence in buffer solution due to fluorescence quenching of the free EB by solvent molecules [69]. However, upon intercalation between the adjacent DNA base pairs, EB emits strongly at 585-590 nm when excited at λ = 525 nm [70]. A competitive binding of another DNA binding molecule could result in the displacement of EB and hence fluorescence quenching [71]. Upon addition of **L** and complexes **1-3** to DNA pretreated with EB, the emission intensity of DNA-EB system decreases, which indicated that the **L** and complexes **1-3** could bind to CT DNA and replace EB, a feature typical of intercalative DNA interactions [72]. The quenching is in agreement with the linear Stern-Volmer equation, which also implies that the **L** and complexes **1-3** bind to DNA (**Fig. 9**).

From the Stern-Volmer equation;

$$I_0/I = 1 + K_{SV} \cdot r$$

Where I_0 and I represent the fluorescence intensities in the absence and the presence of the compound, respectively; r is the concentration ratio of the complex to DNA and K_{SV} is the quenching constant obtained as the slope of I_0/I *vs* r. The K_{SV} values for **L** and complexes **1-3** are 0.67, 0.94, 1.92 and 1.38, respectively suggesting a strong DNA interaction **(Fig 10)**. Moreover, if the compound intercalates in between the DNA base pairs by EB replacement, a new emission peak would emerge at its characteristic wavelength in addition to emission quenching of EB. The emission intensity of the new peak will increase due to the protection from solvent quenching by

ISSN: 2249 –4820

Chemistry & Biology Interface, 2011, 1, 1, 135-160

the hydrophobic region of the DNA. As depicted in Fig. 9b and 9d complexes **1** and **3** behave similarly with the emergence of new emission peak at 570 nm. The emission intensity of EB is decreased where as the emission band at 570 nm is increased, although slightly. These observations imply that the hexa coordinated complexes and the two axial H_2O ligands may lead to rapid electron exchange by electrostatic attractions. The interaction of **1** and **3** with CT DNA may be more classical intercalative binding mode as compared to **L** and **2** which do not exhibit such spectral behavior. The two H_2O ligands of **1** and **3** exert their hydrogen binding affinity to the other regions of the CT DNA helix, facilitating intercalation and also alter the binding capability and electronic transitions [73].

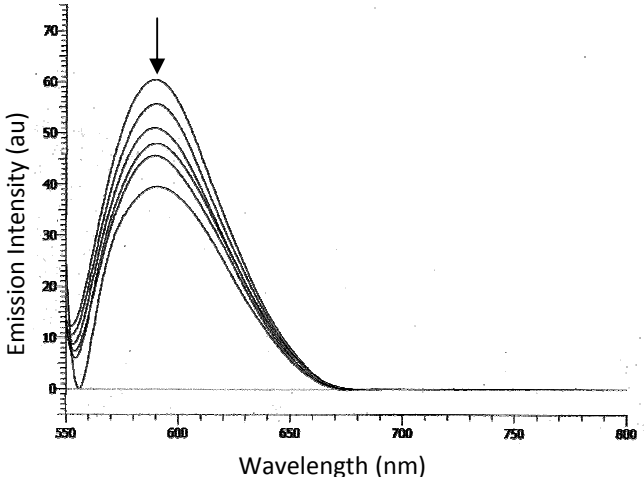

Figure 9a

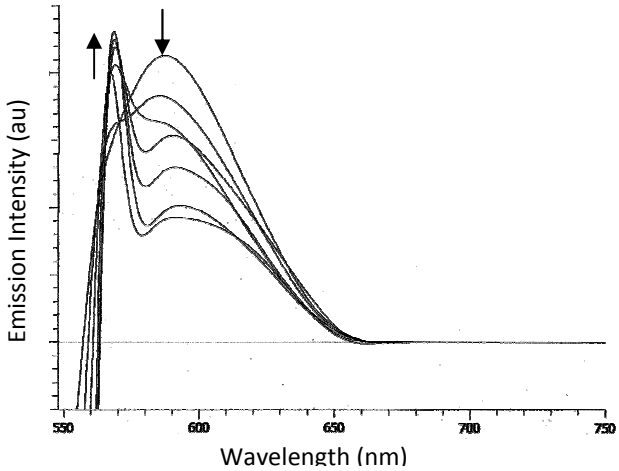

Figure 9b

ISSN: 2249 –4820

Chemistry & Biology Interface, 2011, 1, 1, 135-160

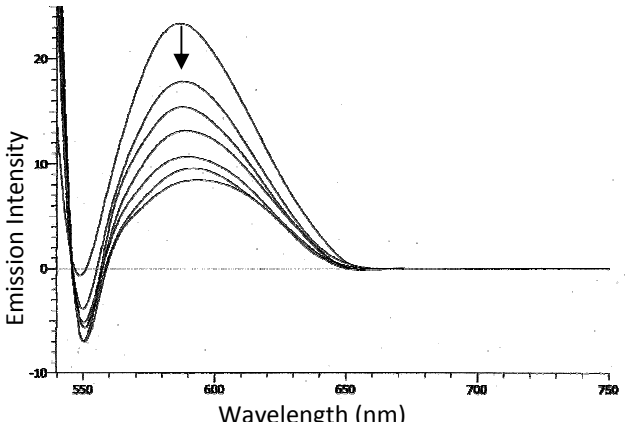

Figure 9c

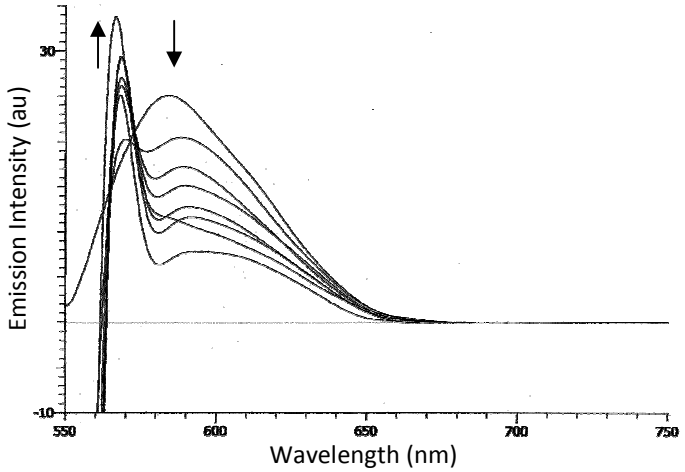

Figure 9d

Emission spectra of EB bound to DNA in the absence and presence of a) ligand **L** b) complex **1** c) complex **2** d) complex **3** in 5 mM Tris-HCl/50 mM NaCl buffer. Arrows show the intensity changes upon increasing concentration of the complexes. [L/Complex] = 3.30 -23.30 μM, [DNA] = 33.00 μM; [EB] = 3.30 μM

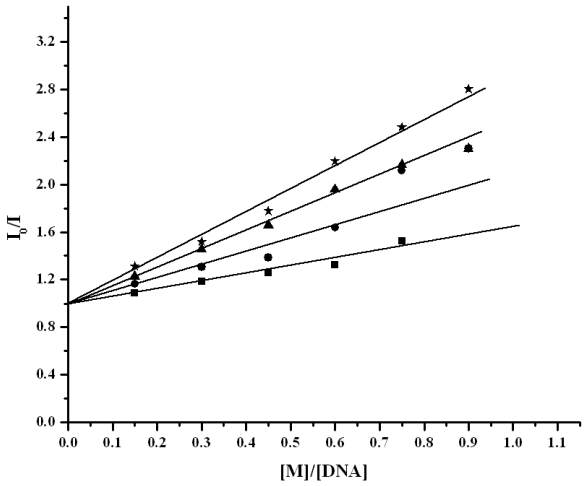

ISSN: 2249 –4820

Chemistry & Biology Interface, 2011, 1, 1, 135-160

Figure 10

Plots of I_0/I against complex concentration. Experimental data points (■, ligand **L**; ●, complex **1**; , complex **2**; ▲, complex **3**); full lines, linear fitting of the data

6. DNA cleavage

The chemical nuclease activity of the complexes **1** and **2** (Fig 11 &12) has been studied using supercoiled pBR322 plasmid DNA as a substrate in a medium of 5 mM Tris-HCl/50 mM NaCl buffer, at pH 7.2 in the absence of an external agent employing gel electrophoresis. The double-stranded plasmid pBR322 exists in a compact supercoiled conformation (SC) Form I.

When subjected to electrophoresis the supercoiled form of DNA is converted into the nicked circular form (NC) Form II and the linear circular (LC) Form III through a single and double strand cleavage, respectively. The fastest migration is observed for supercoiled form while the nicked circular form migrates slowly and the linear form migrates between SC and NC [74]. Hence, the binding of the complexes **1** and **2** with pBR322 plasmid DNA was determined by its ability to change the conformation of DNA from supercoiled (SC) to nicked open circular (NC) form. Different concentrations of complexes **1** and **2** were mixed with the pBR322 plasmid DNA and the mixtures were incubated at 37 ºC for 1h. As depicted in Fig.11a & 12a in absence of any external agents the complexes **1** and **2** scarcely catalyzed the cleavage of plasmid DNA at 10 μM and at 20 μM. When the concentration of the complex was upto 40 μM, the cleavage of SC plasmid DNA into NC form was observed, showing that the cleavage process was concentration dependent. However, no linearized form was observed suggesting a single strand DNA breakage.

To explore the mechanistic pathway of the cleavage activity, comparative DNA cleavage experiments of **1** and **2** were carried out in presence of different additives like ascorbate (Asc) and H_2O_2; standard radical scavengers, DMSO as hydroxyl radical scavenger (HO·), sodium azide (NaN_3) as singlet oxygen ($^1O_2$) quencher and superoxide dismutase as superoxide anion radical ($O_2^{\cdot-}$) scavenger. Figure 11b & 12b indicate little effect on the cleavage efficiency of **1** & **2** in presence of ascorbic acid , DMSO or NaN_3 (lane 2, 4 and 5); suggestive of non-involvement of diffusible (·OH) hydroxyl radicals and singlet oxygen for DNA cleavage. However, superoxide dismutase SOD (lane 6) enhances/promotes the cleavage efficiency in both the complexes. In presence of SOD complex **2** also displayed concomitant conversion of Form II to Form III. The appearance of linearized Form III indicates that the complex **2** is capable of performing double–strand scission of DNA while complex **1** cleaves DNA randomly since linearized DNA was not formed [75]. These observations indicate that $O_2^{\cdot-}$ might be an inhibitor in the plasmid cleavage and reducing the amount of $O_2^{\cdot-}$ can improve the cleavage efficiency [76]. The above observations suggest that the complexes could cleave DNA hydrolytically. Therefore, we propose that the octahedral complexes after intercalation in between the DNA base pairs induce direct coordination of metal ion with the oxygen of the phosphodiester backbone. Subsequently, the electrophilicity of the phosphorus is enhanced making it a suitable target for nucleophilic attack. The activated phosphorus is then attacked by one of the metal-bound water molecules (nucleophile). Due to the intramolecular charge transfer one of the ester bonds of the phosphodiester backbone is broken leading to DNA cleavage [77]. Besides this, the

ISSN: 2249 –4820

Chemistry & Biology Interface, 2011, 1, 1, 135-160

cleavage activity was enhanced in presence of excess of H_2O_2, which suggests that the behavior of the complexes is different from the traditional Fenton-like catalysis as observed for $[Cu(OP)_2]^{2+}$ [78]. Hence, we conclude that the complexes are capable of cleaving DNA by hydrolytic mechanism in absence of H_2O_2 while in presence of the activator H_2O_2 an oxidative pathway may also be operative.

The potential interacting site of complexes **1** and **2** was further explored in presence of the minor groove binder, DAPI and the major groove binder, methyl green. The DNA cleavage activity of **1** and **2** is inhibited in presence of methyl green while it remains unaffected in the presence of DAPI indicating major groove-binding preference of the complexes.

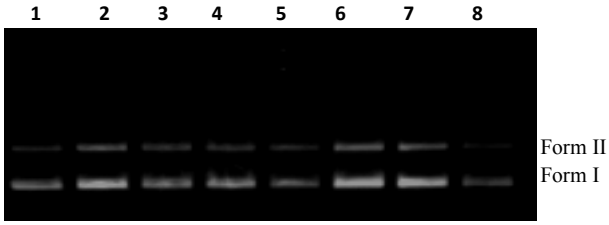

Figure 11a

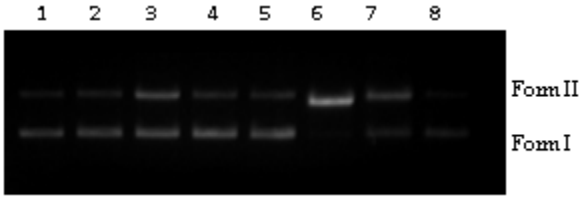

Figure 11b

Gel electrophoresis diagram showing cleavage of pBR322 supercoiled plasmid DNA (300 ng) by (a) complex **1**, control DNA (lane 1),10 μM **1** + DNA, (lane 2), 20 μM **1** + DNA (lane 3), 30 μM **1** + DNA (lane 4), 40 μM **1** + DNA (lane 5), 50 μM **1** + DNA (lane 6), 60 μM **1** + DNA (lane 7), 70 μM **1** + DNA (lane 8); (b) Complex **1** (40 μM) in presence of Asc + DNA, (lane 2), H_2O_2 + DNA (lane 3), DMSO + DNA (lane 4), NaN_3 + DNA (lane 5), SOD + DNA (lane 6), DAPI + DNA (lane 7), MG + DNA (lane 8), control DNA (lane 1).

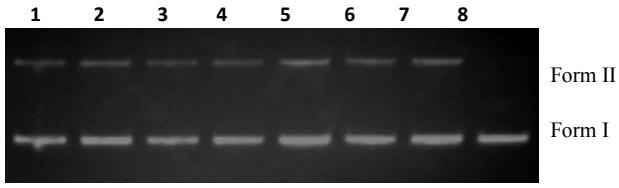

Figure 12a

ISSN: 2249 –4820

Chemistry & Biology Interface, 2011, 1, 1, 135-160

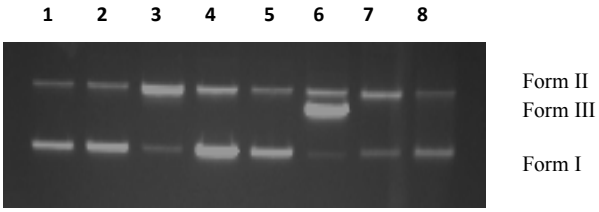

Figure 12b

Gel electrophoresis diagram showing cleavage of pBR322 supercoiled plasmid DNA (300 ng) by (a) complex **2**, control DNA (lane 1), 10 μM **2** + DNA, (lane 2), 20 μM **2** + DNA (lane 3), 30 μM **2** + DNA (lane 4), 40 μM **2** + DNA (lane 5), 50 μM **2** + DNA (lane 6), 60 μM **2** + DNA (lane 7), 70 μM **2** + DNA (lane 8); (b) Complex **2** (40 μM) in presence of Asc + DNA, (lane 2), H_2O_2 + DNA (lane 3), DMSO + DNA (lane 4), NaN_3 + DNA (lane 5), SOD + DNA (lane 6), DAPI + DNA (lane 7), MG + DNA (lane 8), control DNA (lane 1)

7. In vitro cytotoxicity

The *in vitro* cytotoxic and/or the growth inhibitory activity of the ligand **L** and the complexes **1-3** was screened against 14 different human carcinoma cell lines viz; MIAPACA2 (Pancreas), MCF7 (Breast), ZR-75-1 (Breast), SiHa (Cervix), Colo205 (Colon), HOP-62 (Lung), DWD (Oral), K562 (Leukemia), DU145 (Prostrate), A549 (Alveolar), A498 (kidney), A2780 (Ovary), T24 (bladder) and PC-3 (Prostrate). The sulforhodamine-B (SRB) assay was used to assess cellular proliferation [28,79]. The results in terms of GI_{50} values are summarized in the Table 1. The cobalt complex **1** showed the remarkable cytotoxic activity against all cancer cell lines with GI_{50} value <10, while the zinc complex **3** exhibited high cytotoxic activity against MCF7, T24,
MIAPACA2 and DWD cell lines. In comparison to complexes **1** and **3,** the free ligand **L** did not show any significant activity with GI_{50} values > 80 which indicates that the cytotoxicity is enhanced manifold on complexation with metal ions. Surprisingly, the cytotoxicity results do not correlate with DNA binding measurements, where it was found that the complex **2** exhibited higher binding propensity for DNA in terms of intrinsic binding constant K_b and quenching constant K_{sv} than complex **1**. Similarly, complex **2** revealed better cleavage activity. It implicates that the extent of DNA binding and higher cleavage activity is not necessarily the criteria for higher cytotoxicity [80].
Therefore, we propose a hypothesis that complex **1** could induce the conformational change of DNA responsible for its higher cytotoxicity or possibly the complex may bind to the other non-DNA based pharmacological targets viz., proteins or enzymes involved in the cancer profile, [81] which proceed by a different mechanistic pathway involving retardation of different enzymes indispensable for important cellular functions. It is well documented in literature report that conformational changes induced by platinum complexes are directly related to DNA-repair systems and cytotoxic profiles [82]. Our efforts to investigate these possibilities are currently underway.

ISSN: 2249 –4820

Chemistry & Biology Interface, 2011, 1, 1, 135-160

Table 1.

Cytotoxicity against different tumor cells in terms of of GI50 values of ligand **L** and the complexes **1-3.** GI50 ≤ 10 is considered to demonstrate activity

(a)

Cell line	Hop 62	A 549	PC3	DU145	A498	DWD	Colo 205	HT 29
GI_{50} (µg/mL)								
Ligand L	>80	>80	>80	>80	>80	>80	>80	>80
Complex **1**	<10	<10	<10	<10	<10	<10	11.3	<10
Complex **2**	>80	>80	>80	>80	>80	>80	>80	>80
Complex **3**	48.8	62.8	18.2	13.8	31.4	<10	29.6	61.2
Adriamycin	<10	<10	<10	<10	<10	<10	<10	<10

(b)

Cell line	HCT 15	T24	MIA-PA-CA2	MCF7	ZR-75-1	SiHa	HeLa	K562
GI_{50} (µg/mL)								
Ligand L	>80	>80	>80	>80	>80	>80	>77.1	>80
Complex **1**	<10	<10	<10	<10	17.3	<10	<10	40
Complex **2**	>80	>80	>80	>80	>80	>80	>40	>80
Complex **3**	0.5	<10	14.5	10.0	44.9	17.7	34.8	79.7
Adriamycin	<10	<10	<10	<10	<10	<10	<10	<10

- **GI_{50}** Growth inhibition of cancer cell, GI_{50} value was determined from dose–response curve and obtained from three independent experiments
- Yellow highlighted tests indicate activity.

ISSN: 2249 –4820

Chemistry & Biology Interface, 2011, 1, 1, 135-160

8. Conclusion

In this work, we have synthesized and thoroughly characterized metal-based potential drugs possessing pharmacologically active and well-tailored pharmacophore derived from the ligand 3-acetoacetyl-7-methyl-pyrano-[4,3-b]-pyran-2,5-dione. Unlike the ligand, its complexes show a higher binding affinity towards CT DNA. In particular, complex **2** exhibited higher binding propensity with DNA than the complexes **1** and **3**. Surprisingly, complex **1** displayed highest anti-proliferative activity against different human cancer cell lines, while complex **3** was selective for MCF7, T24, MIAPACA2 and DWD cell lines. Thus, the cytotoxicity data did not correlate with simple measurements of DNA binding. Understanding the variation of therapeutic potential *in vitro*, *in cellulo* and *in vivo* is crucial for the development of potential lead antitumour drugs. Alternatively, the profile of complexes on carrier proteins viz. HAS transferrin etc. could throw light on other possibilities of the molecular target (which is currently underway). Furthermore, the complexes warrant *in vivo* testing.

Acknowledgements

We are grateful to the Council of Scientific and Industrial Research, New Delhi (research grant No. 01/(1982)/05-EMR-II) for the financial support. Authors are highly indebted to the Sophisticated Instrumentation Centre, Panjab University, Chandigarh for providing CHN analysis data, ESI-Mass and NMR spectra, Regional Sophisticated Instrumentation Centre, Indian Institute of Technology, Bombay for EPR measurements and ACTREC, Tata Memorial Centre, Mumbai for carrying out the cytotoxic studies.

References

[1] L. Ronconi, P.J. Sadler, Coord.Chem. Rev. **2007**, 25, 1633-1648.
[2] R. Morphy, Z. Rankovic, J. Med. Chem. **2005,** 48, 6523-6543.
[3] H.I. El-Subbagh, S.M. Abu-Zaid, M.A. Mahran, F.A. Badria, M. Al-Obaid, J. Med. Chem. **2000,** 43, 2915-2921.
[4] J.R. Dimmock, V.K. Arora, M.J. Duffy, R.S. Reid, T.M. Allen, G.Y. Kao, Drug Des. Discov., **1992,** 8, 291-299.
[5] G. Kolokythas, N. Pouli, P. Marakos, H. Pratsinis, D. Kletsas, Eur. J. Med. Chem. **2006,** 41, 71-79.
[6] I. K. Kostakis, K. Ghirtis, N. Pouli, P. Marakos, A.L. Skaltsounis, S. Leonce, D.H. Caignard, G. Attasi, Farmaco **2000,** 55, 455-460.
[7] G. Kolokythas, I.K. Kostakis, N. Pouli, P. Marakos, D. Kletsas, H. Pratsinis, Bioorg. Med. Chem. Lett. **2002,** 12, 1443-1446.
[8] S.J. Shaw, H.G. Menzella, D.C. Myles, M. Xian, A.B. Smith III, Org. Biomol. Chem. **2007,** 5, 2753-2755.
[9] M. Grazul, E. Budzisz, Coord. Chem. Rev. **2009,** 253, 2588-2598.
[10] C. Hengeller, G. Licciardelo, V. Tudino, E. Marcelli, A. Virgilio, Nature **1965,** 205, 418- 419.
[11] A. Maxwell, D.M. Lawson, Curr. Top. Med. Chem. **2003,** 3, 283-303.
[12] G.J. Finn, B.S. Creaven, D.A. Egan, Eur. J. Pharm. Sci. **2005,** 26, 16-25.
[13] J.N. Modranka, E. Nawrot, J. Graczyk, Eur. J. Med. Chem. **2006,** 41, 1301-1309.
[14] I. Kostovo, G. Momekov, M. Zaharieva, M. Karaivanova, Eur. J. Med. Chem. **2005,** 40, 542-551.
[15] G. Kokotos, V. Theodoru, C. Tzougraki, Bioorg. Med. Chem. Lett. **1997**, 7, 2165-2168.
[16] I. Manalov, I. Kostova, T. Netzeva, S. Konstantinova, M. Karaivanova, Arch. Pharm. Med. Chem. **2002,** 333, 93-98.
[17] X. Liang, J.A. Parkinson, M. Weishaupl, R.O. Gould, S.J. Paisey, H.S. Park, T.M. Hunter, C.A. Blindauer, S.Parsons, P.J. Sadler, J. Am. Chem. Soc. **2002,** 124, 9105- 9112.
[18] C. Marzano, M. Pellei, F. Tisato, C. Santini, Anti-Cancer Agents in Med. Chem. **2009,** 9, 185-211**.**
[19] V.L. Goodman, G.J. Brewer, S.D. Merajver, Endocr.-Relat. Cancer **2004,** 11, 255-263.
[20] F. Dimiza, A.N. Papadopoulos, V. Tangoulis, V. Psycharis, C.P. Raptopoulou, D.P. Kessissogloua, G. Psomas, Dalton Trans. **2010**, 4517–4528 and references therein.
[21] E.R. Jamieson, S.J. Lippard, Chem. Rev. **1999,** 99, 2467-2498.
[22] J. Marmur, J. Mol. Biol. **1961,** 3, 208-3218.
[23] A. Wolfe, G.H. Shimer, T. Meehan, Biochemistry **1987,** 26, 6392-6396.
[24] G.D. Liu, J.P. Liao, Y.Z. Fang, S.S. Huang, G.L. Sheng, R.Q. Yu, Anal. Sci. **2002,** 18, 391-395.

ISSN: 2249 –4820

Chemistry & Biology Interface, 2011, 1, 1, 135-160

[25] G.D. Liu, J.P. Liao, S.S. Huang, G.L. Shen, R.Q. Yu, Anal. Sci. **2001,** 17, 1031-1036.
[26] V. Rajendiran, M. Murali, E. Suresh, M. Palaniandavar, V.S. Periasamy, M.A. Akbarsha, Dalton Trans. **2008**, 2157-2170.
[27] S. Ramakrishnan, V. Rajendiran, M. Palaniandavar, V.S. Periasamy, B.S. Srinag, H. Krishnamurthy, M.A. Akbarsha, Inorg. Chem. **2009,** 48, 1309-1322.
[28] S.H. van Rijt, A.F.A. Peacock, R.D.L. Johnstone, S. Parsons, P.J. Sadler, Inorg. Chem. **2009,** 48, 1753-1762.
[29] K.S. Siddiqi, F. Arjmand, M. Rehman, S. Tabassum, S.A.A. Zaidi, J. Chem. Research (S), **1994**, 84, J. Chem. Research (M), **1994**, 0383-0393.
[30] B.S. Creavan, D.A. Egan, K. Kavanagh, M. McCann, A. Noble, B. Thati, M. Walsh, Inorg. Chim. Acta **2006,** 359,3976-3984.
[31] Y.S. Kim, S.Y. Park, H.J. Lee, M.E. Suh, D. Schollmeyer, C.O. Lee, Bioorg. Med. Chem. **2003,** 11, 1709-1714.
[32] V. Fargeas, M. Balouch, E. Metay, J. Bafreau, D. Menard, P. Gosselin, J.P. Berge, C. Barthomeuf, J. Lebreton, Tetrahedron, **2004,** 60, 10359-10364.
[33] X.S. Tai, M.Y. Tan, Spectrochim. Acta A **2005,** 61, 1767-1770.
[34] M. Cindric, T.K. Novak, K. Uzarevic, J. Mol.Struct. **2005,** 750,135-141.
[35] H. Khanmohammadi, R. Arabahmadi, M.H. Abnosi, H.R. Khavasi, Polyhedron **2007,** 26, 4963-4970.
[36] I. Yilmaz, H. Temel, H. Alp, Polyhedron, **2008**, 27, 125-132.
[37] S. Ilhan, H. Temel, I. Yilmaz, M. Sekerci, J. Organomet. Chem. **2007,** 692, 3855-3865.
[38] M. Fernandez, R. Bastida, A. Macias, P. Lourido, L. Valencia, Polyhedron **2007,** 26, 5317-5323.
[39] Silverstein, R.M. Webster F.X. Spectrometric Identification of Organic Compounds, 6 Ed. John Wiley India Edition. p173.
[40] S.A. Kotharkar, D.B. Shinde, Bioorg. Med. Chem. Lett. **2006,** 16, 6181-6184.
[41] I. Yavari, M. Bayat, Tetrahedron **2003,** 59, 2001-2005.
[42] K. Abe, K. Atsufuji, M. Ohba, H. Okawa, Inorg. Chem. **2002,** 41, 4461-4467.
[43] Q. Shi, R. Cao, X. Li, J. Luo, M. Hong, Z. Chen, New J. Chem. **2002,** 26, 1397-1401.
[44] M. Scarpellini, A. Neves, R. Horner, A.J. Bortoluzzi, B. Szpoganics, C. Zucco, R.A. Nome Silva, V. Drago, A.S. Mangrich, W.A. Ortiz, W.A. C. Passos , M.C.B. de Oliveira, H. Terenzi, Inorg. Chem. **2003,** 42, 8353-8365.
[45] F. Cisnetti, R. Guillot, M. Desmadril, G. Pelosi C. Policar, Dalton Trans. **2007**, 1473-1476.
[46] H. Kurosaki, R.K. Sharma, S. Aoki, T. Inoue, Y. Okamoto, Y. Suguira, M. Doi, T. Ishida, M. Otssuka, M. Goto, J. Chem. Soc., Dalton Trans. **2001**, 441-447.
[47] D.R. Boer, A. Canals, M. Coll, Dalton Trans. **2009**, 399-414.
[48] I. Kock, D. Heber M. Weide, U. Wolschendorf, B. Clement, J. Med. Chem. **2005,** 48, 2772-2777.
[49] M. Baldini, M.B. Ferrari, F. Bisceglie, P.P. Dall'Aglio, G. Pelosi, S. Pinelli, P. Tarasconi, Inorg. Chem. **2004,** 43, 7170-7179.
[50] T. Yang, C. Tu, J. Zhang, L. Lin, X. Zhang, Q. Liu, J. Ding, Q. Xu, Z. Gou, Dalton Trans. **2003**, 3419-3424.
[51] F. Liu, K.A. Meadows, D.R. McMillin, J. Am. Chem. Soc. **1993,** 115, 6699–6704.
[52] S.M. Hecht, J. Nat. Prod. **2000,** 63, 158-168.
[53] Z.M. Wang, H.K. Lin, Z.F. Zhou, M. Xu, T.F. Liu, S.R. Zhu, Y.T. Chen, Bioorg. Med. Chem. **2001,** 9, 2849-2855.
[54] F. Zhang, Q. Zhang, W. Wang, X. Wang, J. Photochem. Photobiol. A: Chemistry, **2006,** 184, 241-249.
[55] M. Chauhan, K. Banerjee, F. Arjmand, Inorg. Chem. **2007,** 46, 3072-3082.
[56] F. Arjmand, M. Aziz, Eur. J. Med. Chem. **2009,** 44, 834-844.
[57] N.K. Modukuru, K.J. Snow, B.S. Perrin, J. Thota, C.V. Kumar, J. Phys. Chem. B **2005,** 109, 11810-11818.
[58] S. Molz, D.-C. Tharine, H. Decker, C.I. Tasca, Brain Res. **2008**, 1231, 113-120.
[59] I. Sissoeff, J. Grisvard, E. Guille, Prog. Biophys. Mol. Biol. **1976,** 31, 165-199.
[60] V. Andrushchenko, P. Bour, J. Phys. Chem. B, **2009,** 113, 283-291.
[61] M.G. Santangelo, A. Medina-Molner, A. Schweiger, G. Mitrikas, B. Spingler, J. Biol. Inorg. Chem. **2007,** 12, 767-775.
[62] P.P. Neelakandan, M. Hariharan, D. Ramaiah, J. Am. Chem. Soc. **2006,** 128, 11334-11335.
[63] S. van Rijt, S. van Zutphen, H. den Dulk, J. Brouwer, J. Reedijk, Inorg. Chim. Acta **2006,** 359, 4125-4129.
[64] Y. Wang, Z.Y. Yang, Q. Wang, Q.K. Cai, K.B. Yu, J. Organomet. Chem. **2005,** 690, 4557-4563.
[65] X. Xu, K.C. Zheng, L.J. Lin, H. Li, Y. Gao, L.N. Ji, J. Inorg. Biochem. **2004,** 98, 87-97.
[66] J. Liu, H. Chao, Y.X. Yaan, H.J. Yu, L. N. Ji, Inorg. Chim. Acta **2006,** 359, 3807-3814.
[67] B. Wang, Z.Y. Yang, T. Li, Bioorg. Med. Chem. **2006,** 14, 6012-6021.
[68] Z. Li, Q. Yang, X. Qian, Bioorg. Med. Chem. **2005,** 13, 4864-4870.
[69] R.S. Dhar, M. Nethaji, A.R. Chakravarty, J. Inorg. Biochem. **2005,** 99, 805-812.
[70] F.J. Meyer-Almes, D. Porschke, Biochemistry **1993,** 32**,** 4246-4253.
[71] N. Ademir, T. Hernan, H. Rosmari, H. Adolfo Jr, S. Bruno, S. Juliet, Inorg. Chem. Commun. **2001,** 4, 388-391.
[72] C.V. Kumar, J.K. Barton, N.J. Turro, J. Am. Chem. Soc. **1985,** 107, 5518-5523.
[73] C. Rajput, R. Rutkaite, L. Swanson, I. Haq, J.A. Thomas, Chem.-Eur. J. **2006,** 12, 4611-4619.
[74] Y. Masataka, H. Miyako, N. Makoto, M. Keiko, Mol. Genet. Metab. **1999,** 68, 468-472.
[75] C. Tu, Y. Shao, N. Gan, Q. Xu, Z. Guo, Inorg. Chem. **2004,** 43, 4761-4766.
[76] F. Gao, H. Chao, F. Zhou, X. Chen, Y. Wei, L. Ji, J. Inorg. Biochem. **2008,** 102, 1050-1059.

ISSN: 2249 –4820

Chemistry & Biology Interface, 2011, 1, 1, 135-160

[77] J. Tan, L. Zhu, B. Wang, Dalton Trans. **2009**, 4722-4728.

[78] D.S. Sigman, T.W. Bruice, A. Mazumdar, C.L. Sutton, Acc. Chem. Res. **1993,** 26, 98-104.

[79] P. Skehan, R. Storeng, D. Scudiero, A. Monks, J. McMahon, D. Vistica, J.T. Warren, H. Bokesch, S. Kenney, M.R. Boyd, J. Natl. Cancer Inst. **1990,** 82, 1107-1112.

[80] V. Rajendiran, R. Karthik, M. Palaniandavar, H. Stoeckli-Evans, V.S. Periasamy, M.A. Akbarsha, B.S. Srinag, H. Krishnamurthy, Inorg. Chem. **2007,** 46, 8208-8221.

[81] Z. Zang, L. Jin. X. Qian, M. Wei, Y. Wang, J. Wang, Y. Yang, Q. Xu, Y. Xu, F. Liu, Chem Bio Chem. **2007,** 8, 113-121.

[82] Y. Zhao, W. He, P. Shi, J. Zhu, L. Qui, L. Lin, Z. Guo, Dalton Trans. **2006**, 2617-2619.